The Synthesis of Organometallic Coordination Polymer Flowers of Prussian Blue with Ultrathin Petals by Using Crystallization-Assisted Interface Coordination Polymerization (CAICP)

ARTICLE *in* CHEMISTRY - A EUROPEAN JOURNAL · NOVEMBER 2012

Impact Factor: 5.73 · DOI: 10.1002/chem.201202395 · Source: PubMed

6 AUTHORS, INCLUDING:

Tingting Liu
Sun Yat-Sen University
1 PUBLICATION **10** CITATIONS
SEE PROFILE

Guodong Liang
Sun Yat-Sen University
75 PUBLICATIONS **1,143** CITATIONS
SEE PROFILE

Qing wu
Sun Yat-Sen University
197 PUBLICATIONS **3,125** CITATIONS
SEE PROFILE

CHEMISTRY
A EUROPEAN JOURNAL

ChemPubSoc
Europe

DOI: 10.1002/chem.201202395

The Synthesis of Organometallic Coordination Polymer Flowers of Prussian Blue with Ultrathin Petals by Using Crystallization-Assisted Interface Coordination Polymerization (CAICP)

Suping Bao, Tingting Liu, Guodong Liang,* Haiyang Gao, Fangming Zhu, and Qing Wu[a]

The preparation of nanomaterials with well-defined structures has been intensively investigated during the last decade because of their unique structurally dependent properties.[1] The strategies for the synthesis of hierarchical nanomaterials with precisely designed structures are mainly based on templating techniques, in which construction of a proper template is of fundamental importance to the structure and properties of the resulting nanomaterials. Since Mann's group reported the first example of nanocubes of the coordination polymer of Prussian blue (PB) synthesized in reverse microemulsions,[2] a number of worldwide research teams have documented the controlled synthesis of nanoparticles by using various materials as templates. Talham and co-workers have synthesized two-dimensional PB grids by means of the supramoecular assembly of an amphiphilic cyanoferrate derivate at the air–water interface.[3] MacLachlan and coworkers have prepared PB nanoworms and nanocontainers by the assembly of amphiphilic diblock copolymers containing cyanoferrate complexes.[4] Miniemulsion droplets have been used to prepare hollow nanospheres and nanocubes of PB.[5] Very recently, nanocubes of PB with tunable sizes have been synthesized in the presence of polyvinylpyrrolidone and poly(ethylene glycol)-*b*-poly(propylene glycol)-*b*-poly(ethylene glycol).[6] Therefore, it seems evident that new templates may lead to the formation of a catalogue of nanomaterials with unanticipated architectures. Crystallization is a naturally occurring self-assembly process. Anisotropic alignment of polymer chains during crystallization gives rise to the formation of ordered structures, such as lamellae of approximately 10 nm thickness, which offer a new opportunity to generate anisotropic nanoparticles with hierarchical structures. However, templating the growth of nanoparticles by using polymer crystals is unprecedented tothe best of our knowledge.

Herein, we report a facile method to synthesize flower like structures of Prussian blue by using a crystallization-assisted interface coordination polymerization (CAICP) technique. CAICP involves two steps: 1) semicrystalline polymers terminated with the cyanoferrate complex are allowed to crystallize from solution giving rise to flower-like structures; 2) coordination polymerization of the cyanoferrate complex with Fe^{3+} at the solid/liquid interface to generate polymer/PB hybrid flowers (see Scheme 1). Crystallization

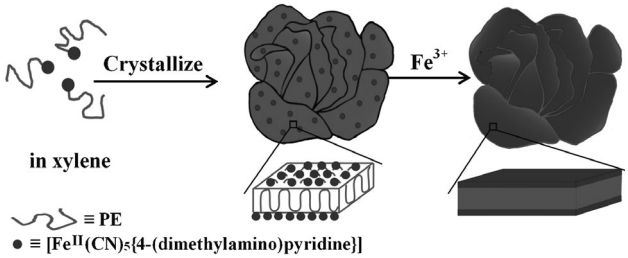

Scheme 1. Schematic illustration of the synthesis of PE-PB hybrid flowers by CAICP.

behavior, which dictates the resulting morphology of polymers, can be well regulated by changing the crystallization conditions including temperature and substrate concentration, making CAICP a powerful method for the fabrication of nanostructures with controlled morphologies. Given the enhanced properties of ordered 3D-flower structures owing to their large surface area and high-index facets,[7] CAICP may open an avenue to a catalogue of new functional nanomaterials with high performance.

To synthesize Prussian blue flowers, semicrystalline polyethylene (PE) terminated by $[Fe^{II}(CN)_5\{4\text{-(dimethylamino)-pyridine}\}]$ (PE-Fe)[8] was dissolved in *para*-xylene (0.1 mg mL^{-1}) at 120 °C with the assistance of sonication, followed by crystallization at 44 °C for 3 h. Upon addition of a solution of Fe^{3+} in methanol, the color of the suspension changed to light blue over a few minutes, indicating the formation of Prussian blue (PB). The observed color change implies that during the crystallization process cyanoferrate

[a] Dr. S. Bao, T. Liu, Dr. G. Liang, Dr. H. Gao, Prof. F. Zhu, Prof. Q. Wu
DSAPM Lab, Institute of Polymer Science, PCFM Lab
OFCM Institute, School of Chemistry and Chemical Engineering
Sun Yat-Sen University
Guangzhou 510275 (P.R. China)
Fax: (+86) 20-84114033
E-mail: lgdong@mail.sysu.edu.cn

Supporting information for this article is available on the WWW under http://dx.doi.org/10.1002/chem.201202395.

complex was expelled from the PE crystals and was relocated to the surface of the PE lamellae, which facilitated the subsequent coordination polymerization with Fe^{3+}. UV/Vis measurements revealed that the addition of small amounts of Fe^{3+} led to the appearance of an absorbance band at 750 nm (Figure S1 in the Supporting Information), which was attributed to the Fe^{II}-CN-Fe^{III} charge transfer.[9] The intensity of the absorbance band increased with the addition of Fe^{3+} until one molar equivalent had been added, which illustrates that Fe^{III} is involved in the reaction. The FTIR spectra of PE-Fe show an absorbance band at 2060 cm^{-1} attributed to the CN stretching vibration. This band shifted to 2072 cm^{-1} after coordination polymerization due to the formation of Fe^{II}-CN-Fe^{III} bridges (Figure S2 in the Supporting Information).[10]

The morphology of PE-PB hybrid flowers prepared by CAICP was characterized by means of scanning electron microscopy (SEM) and transmission electron microscopy (TEM; Figure 1). A typical SEM image illustrates that PE-PB hybrid flowers with a size of about 3 μm consist of self-organized thin petals. The SEM image at higher magnification and a representative TEM image further confirmed the flower like structure with thin petals. Moreover, the petals of PE-PB hybrid flowers have smooth and uniform surfaces, which suggests that continuous rather than isolated PB nanolayers were formed on both sides of the PE lamellae. The thickness of the petals was determined to be 7 nm by measurement of the standing petals observed in the SEM and TEM images, which is close to the fully extended chain length of PE-Fe (Scheme S2 in the Supporting Information).[8] Efforts to acquire energy dispersive X-ray (EDX) elemental mapping and selected-area electron diffraction of PE-PB hybrid flowers were unsuccessful due to the rapid degradation of PE-PB hybrid flowers upon exposure to the electron beam. In addition to PE-PB hybrid flowers with a size of 3 μm, some larger flower aggregates of about 10 μm were also observed. Optical-microscopy images of PE-PB hybrid flowers showed textured structures. Polarizing-optical-microscopy (POM) images of PE-PB hybrid flowers revealed bright stripes in the flowers, which demonstrate the presence of the ordered structures in the polyethylene lamellae (Scheme 1). The EDX spectrum confirmed the presence of iron in the PE-PB hybrid flowers.

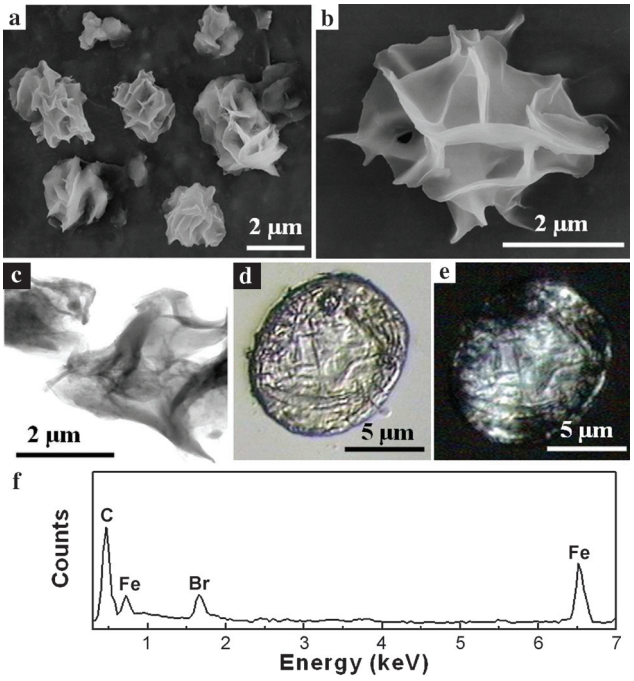

Figure 1. Scanning electron microscopy images a) at low magnification, and b) at high magnification, and c) transmission electron microscopy image, d) conventional optical microscopy image and e) polarizing optical microscopy image of PE-PB hybrid flowers and f) EDX curve from image c.

To verify that the flower like structures were formed by the crystallization of the polyethylene segments, the morphology of PE-Fe after crystallization from solution, but before coordination polymerization with Fe^{3+}, was also examined by SEM (Figure S3 in the Supporting Information). Again, flower-like structures were observed, demonstrating that solution crystallization of PE-Fe was crucial in determining the morphology of the final particles. We also evaluated the effect of cyanoferrate-complex incorporation on morphology. In a control experiment, PE-Br was allowed to crystallize from solution under the same condition as PE-Fe. Disc like rather than flower like structures were observed (Figure S3 in the Supporting Information), which reveals that the cyanoferrate complex is essential to the formation of flower like structures.

Because temperature is a key factor in the crystallization of polymeric materials, PE-Fe was allowed to crystallize at various temperatures to better understand the mechanism of flower formation. Differential scanning calorimetry (DSC) thermograms revealed that the crystallization of PE-Fe from xylene occurred in the temperature range from 40 to 50 °C (Figure S4 in the Supporting Information). Isothermal crystallization of PE-Fe from solution at 50 °C resulted in the formation of parallel-stacked lamellae (Figure S5 in the Supporting Information). Perpendicular stacking of some lamellae was observed when crystallization was carried out at 48 °C. Decreasing the crystallization temperature further to 46 °C gave rise to structures with twisted lamellae radiating from a central lamella. Crystallization at 40 °C resulted exclusively in randomly stacked aggregates. Isothermal crystallization of PE-Fe from xylene was monitored by DSC. A sharp exotherm was observed as a result of isothermal crystallization at 44 °C (Figure S6 in the Supporting Information) and the crystallization halftime was found to be 1.5 min. A broad endotherm was observed at 65 °C in a subsequent heating scan, further confirming that the crystallization of PE-Fe took place.

Crystallization of polymers occurs by nucleation and crystal growth. Crystallization at high temperature is dominated by nucleation, whereas crystal growth is a decisive factor at low temperatures. When PE-Fe is crystallized at higher temperature (50 °C) well-packed lamellae are formed following nucleation as a result of macromolecular rearrangement

stemming from higher molecular mobility at higher temperatures. Decreasing crystallization temperature facilitated nucleation of solvated macromolecules at the cost of crystal growth owing to the lower mobility of macromolecules at lower temperatures. During the crystallization of PE-Fe, the inorganic cyanoferrate complex was expelled from the PE lamellar crystals and subsequently resides on the surface of the PE lamellae. Inorganic layers having high surface energies are inclined to initiate crystallization of macromolecules, which leads to the formation of perpendicular stacked lamellae. Crystallization at lower temperature (40 °C) maximized the nucleation rate, but minimized crystal growth, giving rise to irregular aggregates. Therefore, an optimized crystallization temperature must exist for the formation of PE-Fe flowers at which the rate of crystal growth and nucleation are comparable.

The isothermal crystallization of PE-Fe from xylene at 44 °C was also monitored by dynamic light scattering (DLS). Both particle size and scattering intensity increased gradually with increasing crystallization time (Figure S7 in the Supporting Information). As the crystallization time approached 10 min, both particle size and scattering intensity increased abruptly. This implied that individual PE-Fe lamellae were formed first, and they subsequently self-organized into flowers by aggregation.

We determined the critical micelle concentration (CMC) of PE-Fe in xylene at 120 °C at which polyethylene is soluble, but the cyanoferrate complex is insoluble by means of DLS. DLS results (Figure S8 in the Supporting Information) showed that no particles were detected when the concentration of PE-FE was below 0.1 mg mL^{-1} at 120 °C. The size of the particles formed at a PE-Fe concentration of 0.1 mg mL^{-1} was determined to be 67 nm. Particle size subsequently increased with increasing PE-Fe concentration. Scattering intensity increased rapidly with increasing concentration above 0.1 mg mL^{-1}. Therefore, the CMC of PE-Fe in xylene at 120 °C was determined to be 0.1 mg mL^{-1}.

We also investigated the effect of PE-Fe concentration on the morphology of PB particles. Crystallization from dilute solutions (0.03 and 0.05 g mL^{-1}) gave rise to individual lamellae (Figure S9 in the Supporting Information). Crystallization from solutions with PE-Fe concentrations well above the CMC led to the formation of flowers with thick petals. Crystal growth is dominated by the diffusion of PE-Fe chains towards the crystalline site. High concentrations of PE-Fe in solution expedited crystal growth, leading to the formation of parallel-stacked lamellae and thick petals.

The microstructure of PE-PB hybrid flowers was characterized by X-ray diffractometry (XRD). Two distinct diffraction peaks, ascribed to the (110) and (200) indices of orthorhombic polyethylene crystals, were observed for PE-PB hybrid flowers (Figure S10 in the Supporting Information). No diffraction peaks attributable to Prussian blue crystals were detected in PE-PB hybrid flowers indicating the presence of amorphous PB structures. This is likely a consequence of the nature of the PB nanolayers within the flowers.[5c]

The thermal stability of PE-PB hybrid flowers was tested by means of conventional and polarizing optical microscopy on a hot stage. Optical-microscopy images of PE-PB hybrid flowers showed spherical particles with a finely textured structure. The bright stripes observed in polarizing-optical-microscopy images imply the existence of ordered structures in PE-PB hybrid flowers. PE-PB hybrid flowers kept their shape and contours up to 250 °C, well above the melting temperature of PE (93.5 °C; Figures S11 and S12 in the Supporting Information). In contrast, material examined prior to coordination polymerization with Fe^{3+} shows that PE-Fe flowers collapse after being kept at 180 °C for 30 min (Figure S13 in the Supporting Information), which indicates that the formation of PB layers is a key factor in the improved thermal stability of PE-PB hybrid flowers. The thermal stability of PE-PB hybrid flowers was further evaluated by thermograimetric analysis (TGA). TGA traces for samples of PE, PE-Fe and conventional PB particles were also measured for the purpose of comparison, and are presented in Figure 2. Pristine PE began to decompose at 347 °C with a maximum decomposition rate occurring at 420 °C. The sample had lost 99 % of its mass by the time the sample temperature reached 460 °C. PE-PB hybrid flowers began to lose mass at 427 °C, 80 °C higher than pristine PE. The maximum decomposition rate was reached at 467 °C. PE-PB hybrid flowers retained 40 % of their initial mass, even at

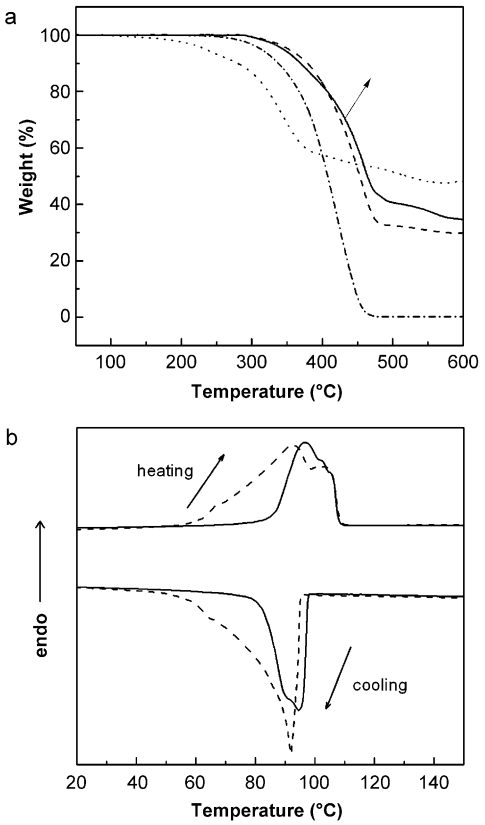

Figure 2. a) TGA and b) DSC traces for samples of PE (–•–•), PE-Fe (-----), conventional PB particles (•••••) and PE-PB hybrid flowers (——).

high temperature (500 °C), thus showing that PE-PB hybrid flowers possess improved thermal stability in contrast to pristine PE. One possible reason for this observation is that sandwiching PE layers between inorganic PB nanolayers in PE-PB hybrid flowers restricts the mobility of PE, which prevents the radical species produced during thermal decomposition from propagating. Moreover, the thermally insulating PB nanolayers tend to inhibit heat flow during degradation.

The freezing and melting behavior of PE-PB hybrid flowers were characterized by DSC (Figure 2b). PE-PB hybrid flowers exhibited narrow freezing and melting peaks in contrast to pristine PE, which illustrates that PE-PB hybrid flowers possess more uniform crystalline structure than PE. Moreover, the freezing and melting temperatures of PE-PB hybrid flowers were 4 and 3 °C higher than those of pristine PE, respectively, which indicates that PB nanolayers helped initiate the crystallization of polyethylene and that PE-PB hybrid flowers have a more crystalline structure than pristine PE.

The PE-PB hybrid flowers fabricated emitted deep-blue light when excited at a wavelength of 350 nm, which is redshifted as compared to conventional PB particles (Figure 3).

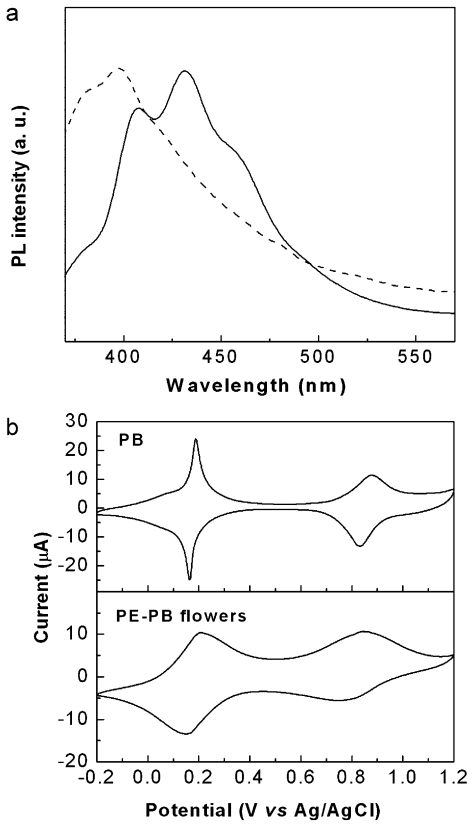

Figure 3. a) Fluorescence spectra and b) cyclic voltammogram of conventional PB particles (-----) and PE-PB hybrid flowers (——). An excitation wavelength of 350 nm was used for fluorescence spectra. For the CV measurements material was deposited on glassy carbon electrodes, and measured in KCl solution (0.1 M), with a scan rate of 50 mV s^{-1} under an N_2 atmosphere.

This redshift is possibly associated with the PB nanolayer structures of flowers.[5b] The electrochemical behavior of PE-PB hybrid flowers was measured by cyclic voltammetry (CV). A typical CV curve for conventional PB showed two sets of distinct redox pairs, one at $E_{1/2}=0.16$ V with a peak separation of 30 mV and one at $E_{1/2}=0.78$ V with a peak separation of 40 mV; these are ascribed to reversible Prussian white/Prussian blue and Berlin green (or Prussian yellow)/Prussian blue conversions, respectively.[11] Both redox pairs were observed with a peak separation of 55 mV for PE-PB hybrid flowers, which implies regular PB structures with homogeneous charge distribution throughout the PB layers. The larger redox peak separation and broad redox peaks observed for PE-PB hybrid flowers are associated with lower diffusion rates of redox species to the electrode, which is likely a consequence of the less ordered structure of the PB layers in PE-PB hybrid flowers in contrast to conventional three-dimensional PB crystals.

In summary, we have developed a conceptionally new method for fabricating PE-PB hybrid flowers with large and ultrathin petals by using a CAICP technique. The petals of the PE-PB hybrid flowers consisted of a single PE layer sandwiched between two amorphous PB nanolayers. TGA results illustrated that PE-PB hybrid flowers exhibited enhanced thermal stability. PE-PB hybrid flowers emitted deep-blue light when excited at a wavelength of 350 nm. CV results revealed that PE-PB hybrid flowers were electrochemically active. The intriguing microstructure of PE-PB hybrid flowers together with their enhanced structure-related properties make them useful in nanodevices, biosensors, and photoluminescent devices, among others.

Experimental Section

Polyethylene terminated with a ferrate complex (PE-Fe) was synthesized by the quarternization of $[Fe^{II}(CN)_5\{4\text{-(dimethylamino)pyridine}\}]$ with mono-bromide-capped polyethylene (PE-Br).[8] For synthesis of PE-PB hybrid flowers, PE-Fe (2 mg) was suspended in *para*-xylene (20 mL) at 120 °C under stirring. The mixture was sonicated for 2 min and stirred for 5 min at 120 °C, followed by quenching to the preset crystallization temperature (40–50 °C). The crystallization duration was fixed at 3 h. PE-Fe concentration in *para*-xylene was in the range of 0.03–0.5 mg mL^{-1}. A solution of $FeCl_3$ in methanol was added to the resulting PE-Fe/xylene suspension. The mixture was stirred overnight at room temperature to give a pale-blue suspension.

Acknowledgements

Financial support by NSFC (21074151), the Guangzhou Planning Project of Science and Technology (11C52050729), the One Hundred Person Project of Sun Yat-Sen University, the SRF for ROCS and SEM, and the Hong Kong Scholar Program (XJ2011047) are gratefully acknowledged. S.P.B. thanks the China Postdoctoral Science Foundation for financial support.

Keywords: crystallization · nanostructures · organometallic compounds · polymerization · Prussian blue

[1] a) H. Goesmann, C. Feldmann, *Angew. Chem.* **2010**, *122*, 1402–1437; *Angew. Chem. Int. Ed.* **2010**, *49*, 1362–1395; b) G. R. Patzke, Y. Zhou, R. Kontic, F. Conrad, *Angew. Chem.* **2011**, *123*, 852–889; *Angew. Chem. Int. Ed.* **2011**, *50*, 826–859.
[2] a) S. Vaucher, M. Li, S. Mann, *Angew. Chem.* **2000**, *112*, 1863–1866; *Angew. Chem. Int. Ed.* **2000**, *39*, 1793–1796; b) S. Vaucher, J. Fielden, M. Li, E. Dujardin, S. Mann, *Nano Lett.* **2002**, *2*, 225–229.
[3] J. T. Culp, J. H. Park, D. Stratakis, M. W. Meisel, D. R. Talham, *J. Am. Chem. Soc.* **2002**, *124*, 10083–10090.
[4] a) X. Roy, J. K. H. Hui, M. Rabnawaz, G. J. Liu, M. J. MacLachlan, *J. Am. Chem. Soc.* **2011**, *133*, 8420–8423; b) X. Roy, J. K. H. Hui, M. Rabnawaz, G. J. Liu, M. J. MacLachlan, *Angew. Chem.* **2011**, *123*, 1635–1640; *Angew. Chem. Int. Ed.* **2011**, *50*, 1597–1602.
[5] a) R. McHale, N. Ghasdian, Y. B. Liu, M. B. Ward, N. S. Hondow, H. H. Wang, Y. Q. Miao, R. Brydson, X. S. Wang, *Chem. Commun.* **2010**, *46*, 4574–4576; b) S. J. Ye, Y. B. Liu, S. J. Chen, S. Liang, R. McHale, N. Ghasdian, Y. Lu, X. S. Wang, *Chem. Commun.* **2011**, *47*, 6831–6833; c) G. D. Liang, J. T. Xu, X. S. Wang, *J. Am. Chem. Soc.* **2009**, *131*, 5378–5379.
[6] a) H. Ming, N. L. K. Torad, Y. D. Chiang, K. C. W. Wu, Y. Yamauchi, *CrystEngComm* **2012**, *14*, 3387–3396; b) M. Hu, S. Furukawa, R. Ohtani, H. Sukegawa, Y. Nemoto, J. Reboul, S. Kitagawa, Y. Yamauchi, *Angew. Chem.* **2012**, *124*, 1008–1012; *Angew. Chem. Int. Ed.* **2012**, *51*, 984–988; c) N. L. Torad, M. Hu, M. Imura, M. Naito, Y. Yamauchi, *J. Mater. Chem.* **2012**, *22*, 18261–18267; d) M. Hu, Y. Yamauchi, *Chem. Asian J.* **2011**, *6*, 2282–2286; e) M. Hu, A. A. Belik, H. Sukegawa, Y. Nemoto, M. Imura, Y. Yamauchi, *Chem. Asian J.* **2011**, *6*, 3195–3199.
[7] a) A. Mohanty, N. Garg, R. Jin, *Angew. Chem.* **2010**, *122*, 5082–5086; *Angew. Chem. Int. Ed.* **2010**, *49*, 4962–4966; b) E. Hao, R. C. Bailey, G. C. Schatz, J. T. Hupp, S. Li, *Nano Lett.* **2004**, *4*, 327–330; c) C. L. Nehl, H. Liao, J. H. Hafner, *Nano Lett.* **2006**, *6*, 683–688; d) J. Xie, F. Zhang, M. Aronova, L. Zhu, X. Lin, Q. Quan, G. Liu, G. Zhang, K. Y. Choi, K. Kim, X. Sun, S. Lee, S. Sun, R. Leapman, X. Chen, *ACS Nano* **2011**, *5*, 3043–3051; e) S. Xiong, J. S. Chen, X. W. Lou, H. C. Zeng, *Adv. Funct. Mater.* **2012**, *22*, 861–871; f) Q. Tian, M. Tang, Y. Sun, R. Zou, Z. Chen, M. Zhu, S. Yang, J. Wang, J. Wang, J. Hu, *Adv. Mater.* **2011**, *23*, 3542–3547.
[8] See the Supporting Information.
[9] a) F. Armand, H. Sakuragi, K. Tokumaru, *New J. Chem.* **1993**, *17*, 351–356; b) S. H. Toma, J. A. Bonacin, K. Araki, H. E. Toma, *Eur. J. Inorg. Chem.* **2007**, 3356–3364.
[10] a) S. F. A. Kettle, E. Diana, E. Boccaleri, P. L. Stanghellini, *Inorg. Chem.* **2007**, *46*, 2409–2416; b) S. Z. Zhan, D. Guo, X. Y. Zhang, C. X. Du, Y. Zhu, R. N. Yang, *Inorg. Chim. Acta* **2000**, *298*, 57–62.
[11] A. A. Karyakin, *Electroanalysis* **2001**, *13*, 813–819.

Received: July 5, 2012
Revised: September 20, 2012
Published online: October 29, 2012

